

Near-Infrared Fiber Optic Temperature Sensor

Christian Schoen, Shiv K. Sharma, Art Seki

Univ. of Hawaii, Hawaii Institute of Geophysics,
School of Ocean and Earth Science Technology (SOEST), Honolulu, HI 96822

Stanley M. Angel

Lawrence Livermore National Laboratory (LLNL)
Environmental Sciences Division, Livermore, CA 94550

ABSTRACT

A series of new fiber optic temperature sensors is proposed. The new design uses the fluorescent emission amplitude of inorganic ions doped in a host matrix in the near infrared region as the temperature determining method and graded index fiber optics as the transmission medium. Four materials are investigated: Er^{3+} :Glass; $\text{Cr}^{3+}, \text{Er}^{3+}$: $\text{Y}_3\text{Sc}_2\text{Ga}_3\text{O}_{12}$; Nd^{3+} : $\text{Gd}_3\text{Sc}_2\text{Al}_3\text{O}_{12}$; and Nd^{3+} :Glass. Feasibility in the design of a 10 km length point sensor with an accuracy of ± 0.2 °C between 0°C and 300°C is presented.

INTRODUCTION

The University of Hawaii (UH) and Lawrence Livermore National Laboratory (LLNL) have an ongoing effort to develop optical fiber sensors (optodes) for in-situ monitoring of physical and chemical parameters in highly corrosive environments such as geothermal wells. As temperature mapping of a geothermal well is important in determining the future production possibilities, we have, in the past, developed and field tested fiber-optic temperature sensors for this application.¹

Temperature sensors developed previously, however, have been limited to a depth of approximately 1 km because of optical losses through the fiber at the visible wavelengths (from 50 dB/km at 488 nm to 15 dB/km at 600 nm). Since many geothermal wells on the Island of Hawaii are ≥ 2 km deep, there is a need to extend these lengths.

In this paper the authors present initial data utilizing the temperature dependence of four near-infrared (NIR) fluorescent materials. By using materials that absorb and fluoresce between 1.0 μm and 1.6 μm , standard graded index communication optical fiber may be used as the transmission medium. Losses using this type of optical fiber at these wavelengths are less than 1.5 dB/km, allowing for the possible generation of a ≥ 2 -km long temperature sensor.

There are a wide variety of available materials that operate in the NIR. Out of forty samples of assorted doped glasses, garnets, and fluoride crystals, four were selected: Er^{3+} :Glass, Nd^{3+} :Glass, $\text{Cr}^{3+}, \text{Er}^{3+}$: $\text{Y}_3\text{Sc}_2\text{Ga}_3\text{O}_{12}$, and Nd^{3+} : $\text{Gd}_3\text{Sc}_2\text{Al}_3\text{O}_{12}$. All four exhibited the strongest fluorescence between 1.3 and 1.55 μm among the group. It was important that the samples fluoresce at wavelengths greater than 600 cm^{-1} from the pump so as not to overwrite the Raman signal generated in the fiber. The importance of this property is discussed below.

Fluorescence properties of all four samples have been previously documented. The fluorescence of Er^{3+} -doped glass was first documented by Snitzer and Woodcock in silicate glass.² The possibility of using a Nd^{3+} laser to pump an Er^{3+} glass laser via absorption by Yb^{3+} sensitizers was first demonstrated by Gaponsev et al.³ The first documentation of Nd^{3+} borate glass fluorescence is reported by Maurer.⁴ The spectroscopy of specialty Nd^{3+} -doped phosphate glass used by LLNL has been reported by Stokowski.⁵ The spectroscopic properties of Er^{3+} and Cr^{3+} -codoped YSGG were first studied by Huber⁶ and later more completely by Moulton.⁷ Finally, the spectroscopy of Nd^{3+} -doped GSAG has been documented by Brandle.⁸

EXPERIMENTAL

A Bomem DA3.02 Model Fourier transform interferometer was used for detection. The FT-Raman machine is equipped with a quartz beamsplitter and a LN₂ cooled InGaAs detector. A single fiber was optically coupled to the 1.06 μm CW Nd:YAG laser beam in 180° scattering geometry (see Figure 1). Except for the Nd:Glass, which was epoxied as a single piece to the end of the fiber, samples were ground to a fine powder, placed in a capillary tube, where the fiber was inserted and buried into the sample. The sample was then placed into a heated oven and monitored by a K type thermocouple attached to a Keithley digital voltmeter. Temperature variations within the oven were measured to be ± 0.2 °C. The entrance end of the fiber was placed into a chuck and inserted into a Newport Corporation Fiber Optic Positioner FP-2 with three degrees of translation. For the Nd³⁺:Glass sample, a 100-meter long step index multimode fiber with a core size of 200 μm and polyimide jacket allowing for temperature measurements of up to 350°C was used in the lab. For the rest of the samples, a 3-meter long fiber was used to investigate the optrode materials.

The fluorescence signal was normalized with respect to the Raman signal of the fiber. The normalized fluorescence intensity thus becomes independent of any fluctuations in the laser intensity.

The Cr³⁺:Er³⁺:YSGG crystal, Nd³⁺:GSAG crystal, and Er³⁺:Glass all required a 1.0 OD filter in the return path (after the elliptical mirror) in order that the fluorescence did not saturate the detector. The Er³⁺:Glass showed such strong fluorescence, a KG1 filter producing 30 dB attenuation at 1.06 μm had to be used on the pump laser since its 50 mW threshold energy at 1.0641 μm (9397.6 cm⁻¹) output could not be reduced. This reduced the pump energy to 0.05 mW to the Er³⁺:Glass sample. In the cases of the Er³⁺, Cr³⁺:YSGG and the Nd³⁺:GSAG, the energy to the sample was 50 mW.

RESULTS

The Er³⁺-doped phosphate glass sample from Kigre Inc. is codoped with Yb³⁺ ions, which act as a fluorescence enhancer since the Yb³⁺ exhibits strong absorption at 1.06 μm and then transfers this energy to the ⁴I_{11/2} band of Er³⁺ ion through nonradiative energy transfer. Fluorescence at 1.54 μm is caused by a radiative transfer from the ⁴I_{13/2} metastable state to the ⁴I_{15/2} ground level. Figure 2 shows the Er³⁺:Glass fluorescence spectra variation with temperature ranging from room temperature to 225 °C. Figure 3 shows the normalized fluorescence amplitude variation as a function of temperature. The experimental data points are curve fit to a first order polynomial. The slope of the normalized amplitude as a function of temperature is 0.1/°C over the temperature range monitored.

The fluorescence amplitude temperature dependence of Nd³⁺-doped (2 to 3% by weight) phosphate glass from the LLNL NOVA laser was examined. Nd³⁺-doped phosphate glass exhibits fluorescence at 7545 cm⁻¹ (1.3 μm) which is a result of the radiative transfer from the ⁴F_{3/2} to the ⁴I_{13/2} energy levels. Figure 4 shows the fluorescence spectra variation with temperature from 0 to 100°C. Figure 5 shows the normalized fluorescence amplitude variation as a function of temperature. The slope is 0.04/°C.

The fluorescence spectra of Er³⁺,Cr³⁺:YSGG at room temperature is shown in figure 6. The 1.53 μm fluorescence results from the radiative decay of the ⁴I_{13/2} metastable level to the ⁴I_{15/2} ground level. A plot of the normalized amplitude as a function of temperature is shown in Figure 7. As opposed to the other two samples, Er³⁺,Cr³⁺:YSGG decreases in amplitude with an increase in temperature. The experimental data points were curve fit to a first order polynomial. The slope of the normalized amplitude as a function of temperature is -0.007/°C.

The fluorescence spectra of Nd³⁺:GSAG at room temperature is shown on figure 8. The 1.32 μm fluorescence peak results from the radiative transfer of the ⁴F_{3/2} metastable level to the ⁴I_{13/2} state.^{8,9} A plot of the normalized amplitude as a function of temperature is shown in Figure 9. The experimental data points were curve fit to a second order polynomial. The slope of the normalized amplitude as a function of temperature is 0.016/°C.

DISCUSSION

As opposed to the other three samples, $\text{Er}^{3+}, \text{Cr}^{3+}:\text{YSGG}$ exhibited a decrease in fluorescence amplitude as a function of increasing temperature. This can be attributed to the fact that the $1.53 \mu\text{m}$ fluorescence is terminated at the ground level. As the temperature increases, the ground level is depopulated, allowing a greater chance for other radiative or nonradiative transfers to occur.

As opposed to the $\text{Nd}^{3+}:\text{GSAG}$ exponential increase in amplitude as a function of increasing temperature, the Nd^{3+} -doped glass responds to temperature with a linear increase. This most likely can be attributed to the fluorescence being predominantly thermally assisted and not a function of the weak absorption at $1.06 \mu\text{m}$.

Table 1 compares the results of the four materials used as possible temperature optrode materials. The first column compares the slope of the normalized amplitude response. The greater the slope, the more sensitive the material is to temperature. Er^{3+} -doped glass proves to be the most sensitive with a $0.1/^\circ\text{C}$ sensitivity. This is almost 2.5 times greater than the next sensitive material, the Nd^{3+} -doped glass. The second column of table 1 shows the computer curve fit calibration. In generating an optical temperature sensor with a computer interface, the calibration curve must fit the experimental data points if an accurate temperature is to be determined. The three materials measured were all much less than the $\pm 0.2^\circ\text{C}$ calibration error.

CONCLUSION

Four different materials that absorb and fluoresce in the NIR are compared as possible NIR temperature optrode materials. Er^{3+} -doped phosphate glass proves to be the most sensitive medium. Future work will concentrate on incorporating the Er^{3+} -doped phosphate glass into a fully remote temperature monitoring system for long-length geothermal well temperature mapping.

ACKNOWLEDGMENTS

Special thanks to Kigre Inc. for its Er^{3+} -doped phosphate laser glass. Also thanks to Allied Inc. for its samples of $\text{Er}^{3+}, \text{Cr}^{3+}:\text{YSGG}$ and $\text{Nd}^{3+}:\text{GSAG}$. We would like to thank Dr. Patrick Takahashi and Dr. Harry Olsen of HNEI for their support and encouragement. This is SOEST contribution No. 2636.

REFERENCES

1. Angel, S. M., D. G. Garvis, S. K. Sharma and A. Seki, "Field Applications of Fiber-Optic Sensors. Part I: Temperature Measurements in a Geothermal Well," *Applied Spectroscopy* 43(3), 430-435 (1989).
2. Snitzer, E., R. Woodcock, " $\text{Yb}^{3+}-\text{Er}^{3+}$ Glass Laser," *Appl Phys Lett* 6, 45-46 (1966).
3. Gapontsev, V. P., M. E. Zhabotinskii, A. A. Izyneev, V. B. Kravchenko and Y. P. Rudnitskii, "Effective $1.054 \mu\text{m}$ to $1.54 \mu\text{m}$ Stimulated Emission Conversion," *JETP Lett.* 18, 251 (1973).
4. Maurer, R. D., "Operation of a Nd^{3+} Glass Optical Maser," *Applied Optics* 2(1), 87 (1963).
5. S. E. Stokowski, R. Saroyan, and M. Weber, *Nd-Doped Laser Glass Spectroscopic and Physical Properties*, Lawrence Livermore National Laboratory, Livermore, Calif., M-95 Rev. 2, 5019 (1981).
6. Huber, G. and E. W. Duczynski, "Cr-Sensitized Rare Earth Garnet Lasers at Room Temperature." *Journal de Physique*. C7, C7-309-313 (1987).

7. Moulton, P. F., J. G. Manni and G. Rines, "Spectroscopic and Laser Characteristics of Er,Cr:YSGG." IEEE Journal of Quantum Electronics. 24(6), 960-973 (1988).
8. Brandle, C. D., J. C. Vanderleeden, "Growth, Optical Properties, and CW Laser Action of Neodymium-Doped Gadolinium Scandium Aluminum Garnet," IEEE Journal of Quantum Electronics, QE-10(1), 67-70 (1974).
9. Kaminski, A. A., Laser Crystals. Springer-Verlag. Berlin, Springer-Verlag (1981).

	Temperature Response Slope (1/°C)
Er:Glass	0.1
Nd:Glass	0.04
Cr,Er:YSGG	-0.007
Nd:GSAG	0.016

Table 1. Comparison of material sensitivity and accuracy as a temperature sensor.

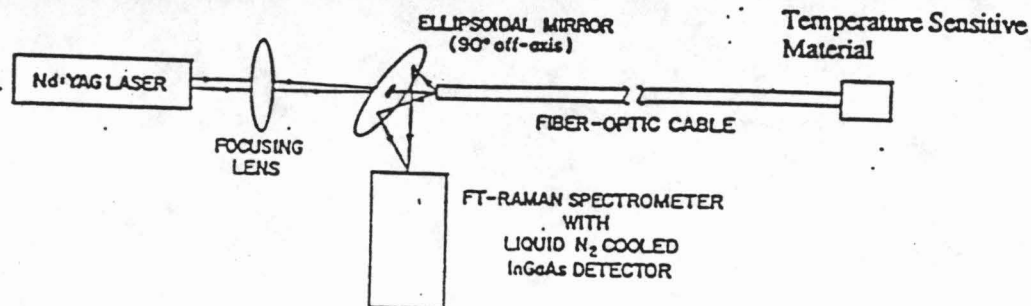


Fig. 1. Schematic diagram showing the experimental setup for an extended length near-IR fluorescence temperature sensor.

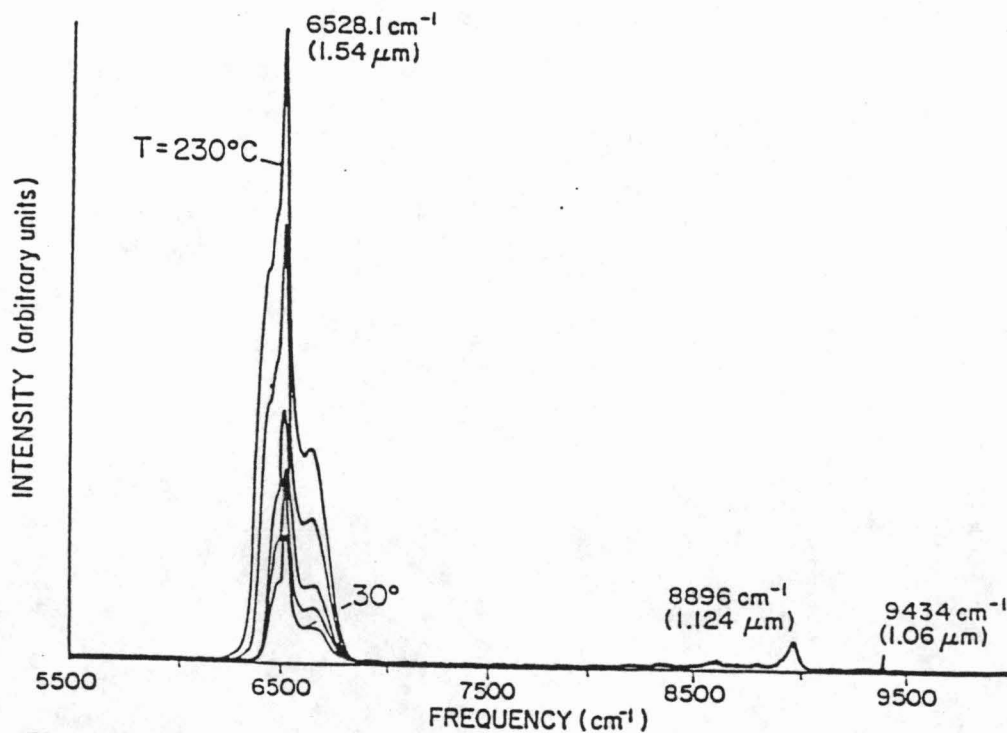


Fig. 2. Effect of temperature on the 1.54 μm fluorescence band of a Er doped phosphate glass temperature optrode excited at the end of an optical fiber with 1.06 μm laser radiation.

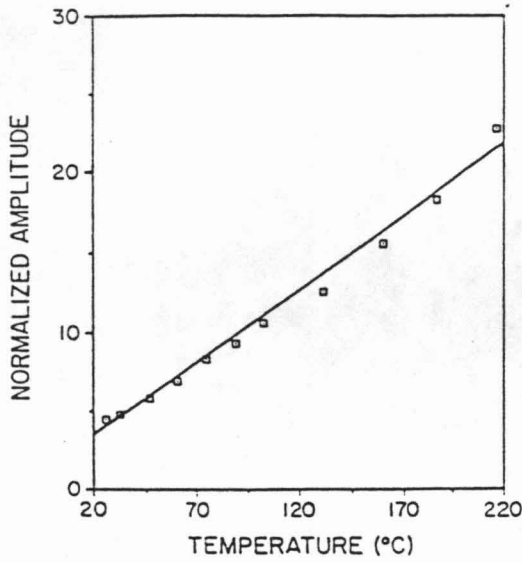


Fig. 3. Normalized fluorescence amplitude response curve as a function of temperature for Er doped glass optrode. Experimental data are marked as points. The first order curve fit is shown as a solid line and is represented by: Normalized Amplitude (NA) = $1.3745 + 9.2380 \times 10^{-2}(T)$; $R^2=0.987$.

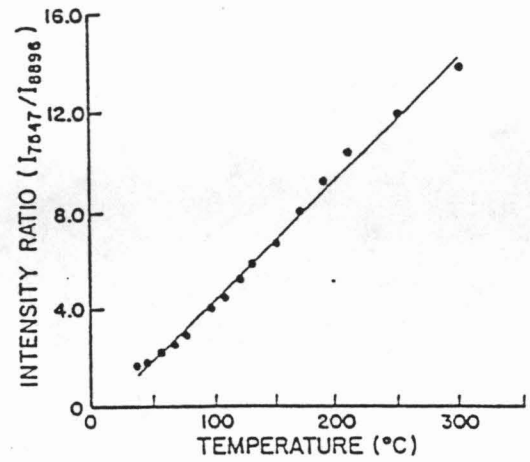


Fig. 5. Calibration curve in the range 25 to 350°C using a 100 meter long optical fiber. Intensity ratio is the ratio of intensities of 8896 cm^{-1} fluorescence band of Nd to that of the silica Raman band of the fiber at 8896 cm^{-1} .

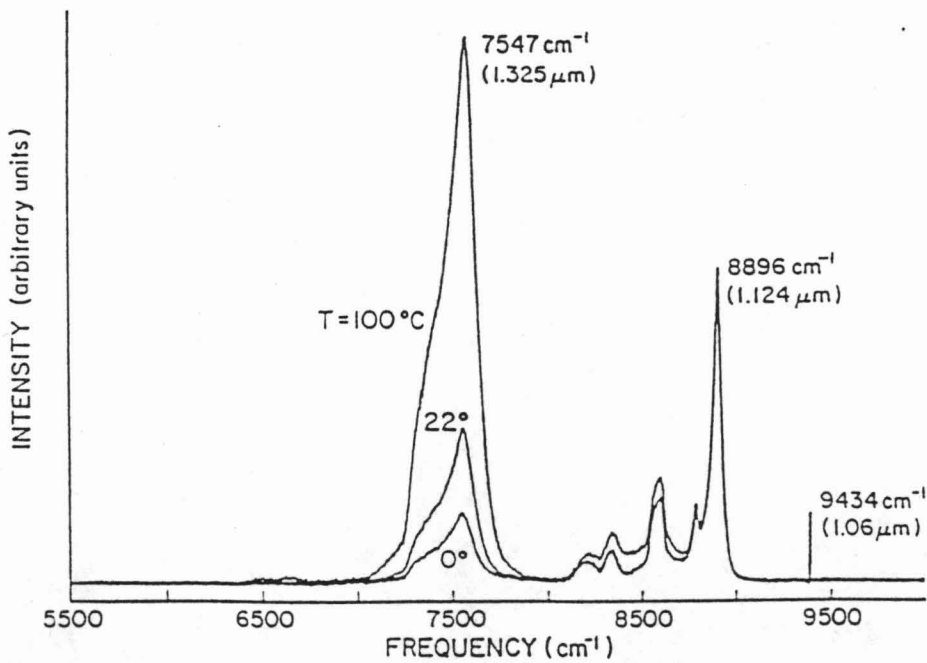


Fig. 4. Effect of temperature on the 1.3 μm fluorescence band of a Nd doped phosphate glass temperature optrode excited at the end of a 100 meter long optical fiber with 1.06 μm laser radiation.

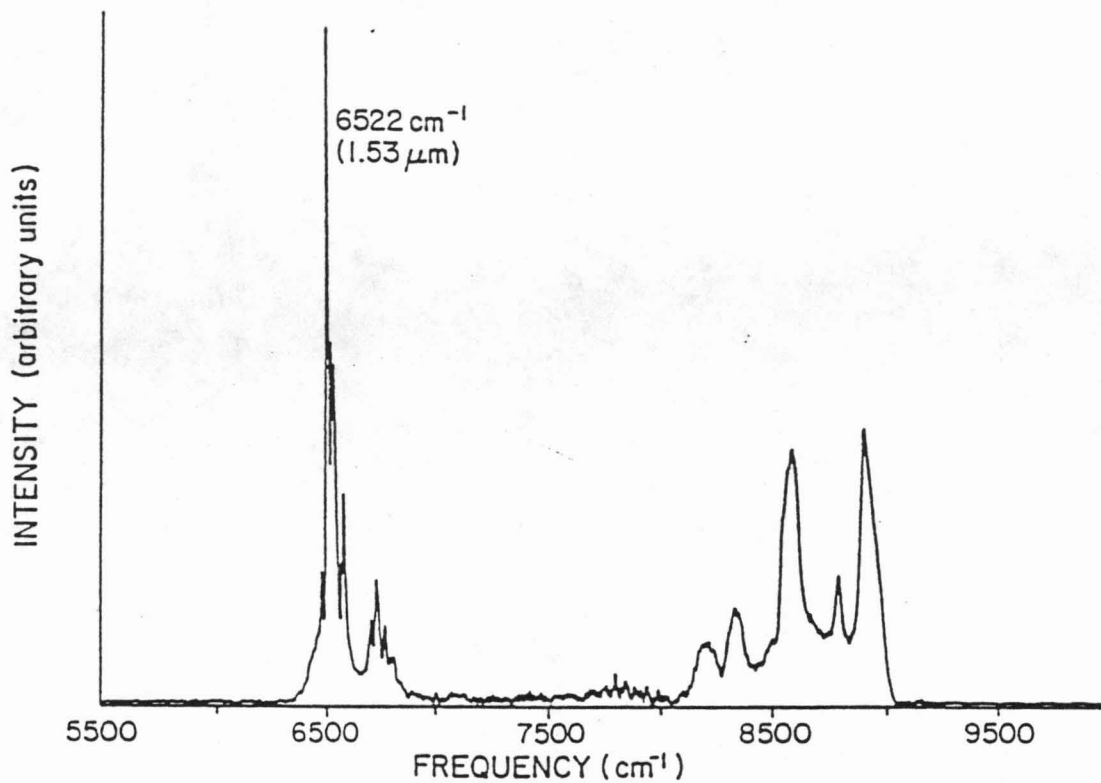
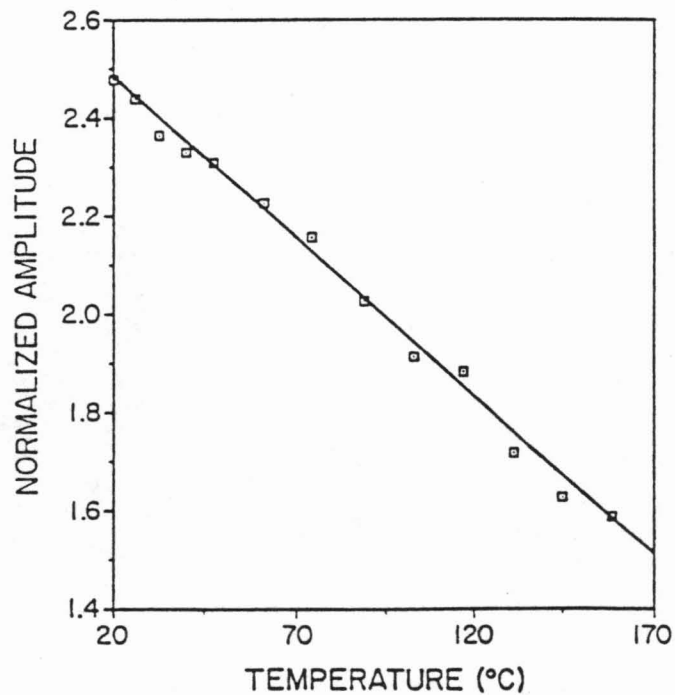


Fig. 6. Fluorescence spectra of Er, Cr codoped YSGG at room temperature excited at the end of an optical fiber incident with 1.06 μm laser radiation.

Fig. 7. Normalized fluorescence amplitude response curve as a function of temperature for Cr, Er doped YSGG opmode. Experimental data are marked as points. The first order curve fit is shown as a solid line and is represented by: Normalized Amplitude (NA) = $2.5996 - 6.4202e-3(T)$; $R^2 = 0.995$.



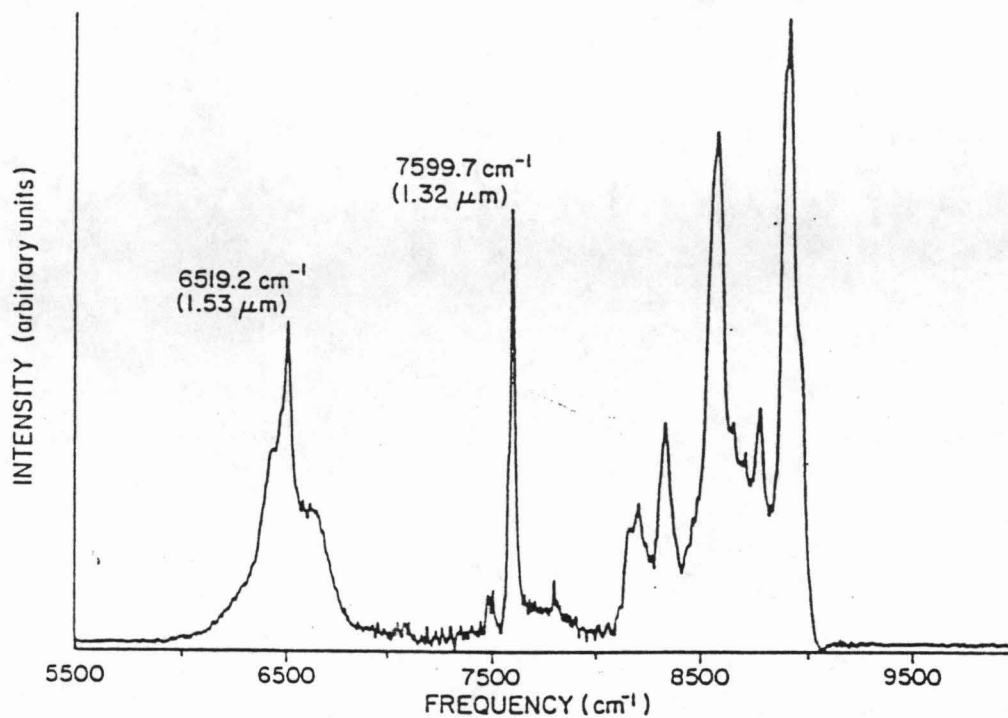


Fig. 8. Fluorescence spectra of Nd doped GSAG at room temperature excited at the end of an optical fiber incident with 1.06 μm laser radiation.

Fig. 9. Normalized fluorescence amplitude response curve as a function of temperature for Nd doped GSAG optrode. Experimental data are marked as points. Second order curve fit is shown as a solid line and is represented by: Normalized Amplitude (NA) = $0.20430 + 1.6423e-4(T) + 7.60636e-5(T^2)$; $R^2 = 0.999$.

